

Thermal comfort in residential buildings with water based heating systems: a tool for selecting appropriate heat emitters when using μ -cogeneration.

Leen Peeters¹, Nicolas Kelly², William D'haeseleer¹

¹ Applied mechanics and Energy Conversion, University of Leuven (K.U.Leuven), Belgium

²Energy Systems Research Unit, University of Strathclyde, UK

ABSTRACT

As a consequence of people becoming more aware of their impact on the environment, there is an increasing demand for low energy buildings. Forced by regulation, building envelopes are improving and heating and cooling systems with higher efficiencies are being installed. The public are willing to embrace these new technologies, as long as they do not affect the quality of their indoor environment.

In this paper, an introduction to research on the realisation of the indoor thermal comfort in residential buildings with water based, low-energy heating systems is given. The basis for this work is a more realistic definition of comfort temperatures for residential buildings. Subsequently, appropriate heat emitters to realise that thermal comfort in an efficient way are identified, taking into account the limitations of the production system under consideration. An example of a μ -cogeneration system is presented as a case study.

INTRODUCTION

A low energy buildings could have significantly reduced energy losses to the outdoor environment compared to normal dwellings, making them more susceptible to variations in temperature due to indoor energy fluxes. Despite the radically different thermal characteristics of these dwellings, conventional water based heat emitters (e.g. radiators and floor heating) continue to be installed in them. The research reported in this paper assesses if these more conventional heat emitters can achieve adequate thermal comfort in low energy dwellings. Further, if the heat emitters need to be replaced, the characteristics of better suited heat emitters and a suitable heat production system are identified. This is effectively an optimization problem and the approach taken to tackle this problem is shown in Figure 1.

The starting point is the achievement of thermal comfort in the dwelling with minimum energy consumption. This is then mapped to appropriate heat

emission technology and ultimately the heat production technology. However, the heat production system has certain characteristics which might limit the heat outcome; maximum capacity, lock out time, etc. This will influence the heat emission and, in turn, might make other heat emitter characteristics more suitable to realise the desired indoor thermal comfort, and so on.

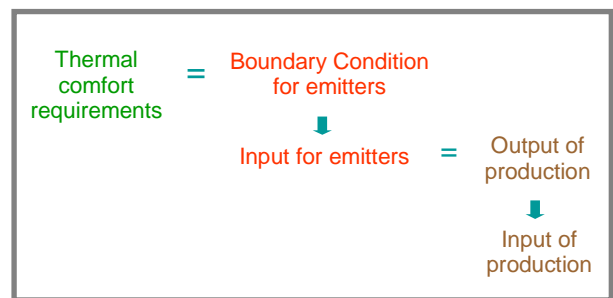


Figure 1: Reconsidering the heating equipment for low energy buildings.

This paper presents the software that has been developed to assist in the optimization of the heating installations for low energy buildings. A case study is presented which focuses on matching heat emitters to two different μ -cogeneration systems: Internal Combustion Engines (ICE) and boiler-Stirling Engines (SE). The outcome of the process will be the compatible heat emitter's characteristics. Another outcome of the process is the emitter characteristics to be avoided.

The constraint for the optimization process is that thermal comfort conditions are achieved with minimum energy consumption.

METHODOLOGY

Thermal Comfort

If effective optimization is to be achieved it is important that appropriate thermal comfort criteria are selected. The important question is which criteria are suitable for low energy dwellings?

Many different standards and theories for thermal comfort have evolved since Fanger published his seminal thermal comfort theory [Fanger, 1970], based on environmental and physiological parameters such as the air speed and the air temperature and parameters of the individuals under consideration (e.g. clothing and metabolic rate). Fanger introduced the terms Predicted Mean Vote¹ (PMV) and Percentage of People Dissatisfied² (PPD).

Whilst Fanger's work is appropriate for near steady state indoor conditions such as those experienced in offices and office-like environments, it is less appropriate for residential buildings where the inhabitants have a wide range of possibilities to adapt themselves to a dynamic thermal environment by opening windows, changing clothing or activity level and going to another room.

The recently renewed International Standard ISO 7730 [ISO, 2005] uses these PMV- and PPD- indexes to predict the thermal sensation of people exposed thermal environments where moderate deviations from steady state occur. When considering cases where the occupants have many ways to adapt themselves or the environment to achieve a more agreeable thermal sensation, the ISO standard suggests using a wider PMV range. However, this vague notion of a wider PMV range does not provide an adequate comfort metric for residential buildings.

The standard 55-2004 set up by ASHRAE [ANSI/ASHRAE 55-2004] is a revision of the former ASHRAE 55-1992 standard. Like ISO 7730, the new standard uses PMV- and PPD-indices. However, it also determines the values of acceptable temperature changes per time interval, and in that way it partly accounts for the dynamic effects ignored by both Fanger and ISO 7730. However, the standard is still based on the PMV- and PPD-indices, which are based on steady state experiments in climate chambers and are not particularly appropriate for the more dynamic conditions experienced in dwellings.

The recently defined Adaptive Temperature Limits (ATL) method specifies two kinds of buildings; free running buildings, α -types, and air conditioned buildings or β -types [Van der Linden et al., 2006]. It is specifically stated that residential buildings could be considered as α -buildings. The ATL gives an indoor temperature comfort range as a function of the reference outdoor temperature $T_{e,ref}$, which varies

according to the current and previous days' temperature characteristics. This is given by Equation 1.

$$T_{e,ref} = \frac{(T_{today} + 0.8T_{today-1} + 0.4T_{today-2} + 0.2T_{today-3})}{1 + 0.8 + 0.4 + 0.2} \quad \text{Equation 1}$$

where

$T_{e,ref}$ = Reference external temperature (in °C)

T_{today} = Average of today's maximum and minimum external temperature (°C)

$T_{today-n}$ = Average of the maximum and minimum external temperature (°C) of n days ago

This method shows some agreement with the little experimental data on residential buildings available in the literature [Oseland, 1994; Oseland 1995; Janssens and Vandepitte, 2006].

The research reported in this paper uses a slightly modified version of ATL to account for the observations of De Dear [De Dear et al., 1997] who observed a lower sensitivity to indoor temperature changes in case of residential buildings compared to free running office buildings. This results in an asymmetric comfort temperature distribution around a neutral temperature, shown in figure 2. The concept of an asymmetric distribution of the comfort band around the neutral temperature is also discussed by Humphreys and Hancock [Humphreys, Hancock, 2007], and Fountain et al. [Fountain et al. 1996].

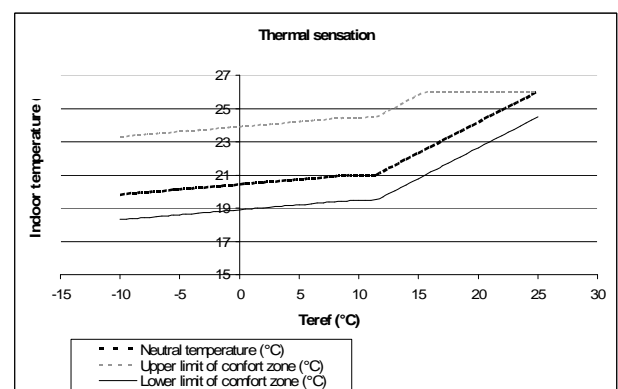


Figure 2: Comfort temperature and upper and lower limits of 10% PPD-zone as a function of $T_{e,ref}$.

The asymmetric comfort temperature distribution is valid for the rooms with activity and clothing levels similar to those found in dwellings and offices. However, it does not agree with experimental data for bathroom(s) and bedrooms. Specific guidelines will be

¹ The PMV predicts the actual thermal sensation of an average person in a given thermal environment.

² The PPD gives the percentage of possible complainers.

set up for these rooms, but their derivation is outside the scope of this paper.

Strategy

Now that an appropriate comfort metric has been defined, the next step in implementing the heat emitter optimization process of Figure 1 is to integrate the comfort metric and modified algorithms, into a building energy simulation (BES) code..

The BES-program that is opted for is ESP-r [ESRU, 2007]. This code solves the building and its constituents simultaneously and in the transient domain [Jensen, 1993]. All aspects of the model, building as well as plant, are considered as a collection of small finite volumes. These represent the various regions of both building and plant between which energy and mass can flow (figure 3). For each of these finite volumes, at each simulation time step, the conservation laws of mass, energy and momentum can be applied resulting in coupled equations representing the processes in the finite volumes.

These equations are passed on to the central numerical solver where they are regrouped in sub-sets, according to the physical process they represent. Several solvers, specifically developed for each sub-set, work in tandem to solve the overall problem. The boundary conditions for this solution are provided by the climate data selected by the user and by user selected or defined control criteria. [Clarke, 2001; Kelly 1998].

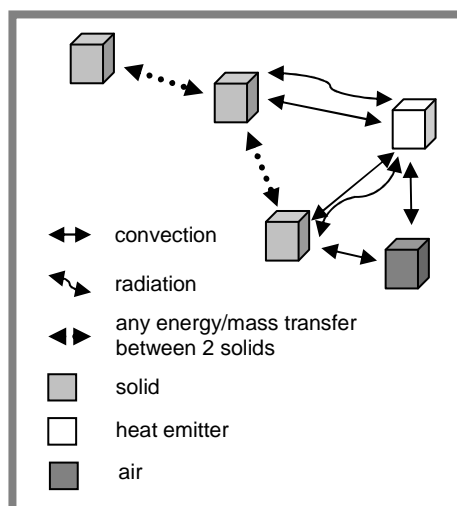


Figure 3: Finite volumes, representing interactions between a heat emitter, some solid structure and zone air.

In ESP-r any space within a building model will interact with a heat emitter through a combination of conduction, convective and radiant heat exchanges. Heat can be injected into any finite volume within the

zone of interest. It is therefore possible to model any type of emitter in an abstract fashion. Note that the same process can be used to represent cooling devices. This abstract representation of heating/cooling devices coupled with a control algorithm and sensor is collectively termed a “control function” within ESP-r. Control functions can be used as a simple way to represent the action of plant and systems within a building without resorting to detailed plant modelling. The tool incorporates many different types of function allowing the modeller to represent many different types of systems interaction: from ideal control of user defined environmental parameters through to fuzzy-logic based control.

For the purpose of this paper, one of ESP-r’s control functions has been adapted to include the user defined emitter characteristics and constraints such as the percentage of radiant and convective heat transfer, maximum capacity and a time constant which indirectly represents emitter thermal mass. The algorithm also has the ability to operate with the modified ATL comfort algorithm and asymmetric bounds around the indoor comfort temperature described previously. Using this approach a radiator can be modelled as a mixed radiant/convective heat injection into a zone with a small time constant. This can be converted to a floor heating system simply by changing the radiant convective split and the time constant of the emitter.

This modified algorithm (hereafter termed a “zone controller”) can therefore be used to represent specific emitter characteristics for individual zones within a building.

A further algorithm has been developed as an abstract representation of the heat production equipment (in this case μ -cogeneration). This is termed a “global controller”, which represents the state of the heating plant and governs the operation of one or more zone controllers (i.e. the heat emitters connected to the central plant).

The advantage of this abstract modelling approach is that it is easy to apply an external optimization code to the simulation process. The characteristics of the emitters and heat supply system can be radically altered simply by changing data parameters in the appropriate controllers. A more detailed model would require significantly more intervention and adaptation of the model.

Implementation and Operation

The zone and global controller algorithms have been implemented within ESP-r. Each zone controller uses

the sensed operative temperature (a mix of 50% mean radiant temperature and 50% air temperature [Hens, 1995].) as an input. The comfort temperature is then calculated for the zone (e.g. a living room, kitchen, etc.) using the modified ATL algorithm. Using the constraint of the emitter maximum capacity and time constant, the desired energy flux is calculated. This final value of the desired zone energy flux is passed on to the global controller. Once all of the individual zone controller heat flux requirements have been calculated, the global controller checks the maximum and minimum installed power and, if necessary, rescales the energy available to each emitter. Other constraints that will affect the availability of heat are also accounted for; these include user-defined lock out times, minimum on-time or possible forced part load time³. Finally, temporal system start up and shut down effects are taken into account. The modified energy fluxes are then passed back to the individual zone controllers and injected into each zone according to the user defined heat emitter characteristics. This reasoning is shown in Figure 4: the zones require some energy, the amount they can get after taken into account possible restrictions due to the zone controller, is passed on to the global controller. There, it is checked with constraints that might have been built in the logic of the global controller. Eventually the allocated energy is calculated.

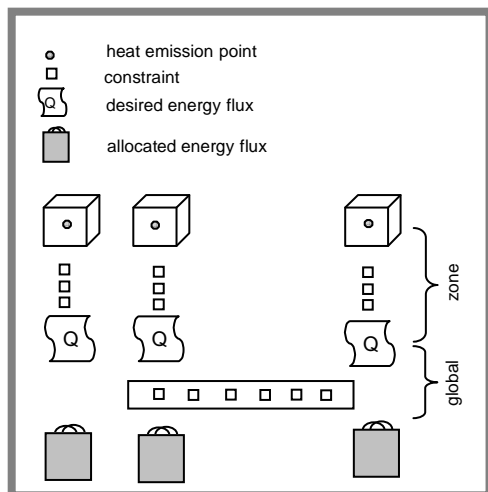


Figure 4: The order of constraints in case of a global controller.

³ Modulating heat producing devices can have a fixed time at start up during which they work on part load.

This is implemented to achieve a stable condition in the cogeneration unit.

Case study

The objective of this case study is to analyse the performance of two different μ -cogeneration devices in a residential building and to formulate suggestions for the appropriate heat emission elements they should be combined with under different operating conditions. In this case the residential building is modeled as a single zone.

The climate boundary conditions are provided by an abstract climate file that has been devised to help determine the influence of the outdoor temperature on heating system performance. This file consists of blocks of 18 days with constant temperature, increasing from -10 °C up to 30 °C in steps of 2 °C. Other climate data such as solar radiation and wind speed are set to constant average values.

The target for the heating system is to maintain an indoor thermal comfort condition that is within the limits of 10% dissatisfied people as calculated using the modified ATL algorithm. The characteristics of the heat emitter used in the model are varied as follows;

$$\tau_e : 1 - 50 - 100 - 500 - 1000$$

$$conv : 10 - 25 - 50 - 75 - 99$$

where τ_e is the emitter time constant (s) and *conv* indicates the percentage of convective heat emission. (1-*conv*) thus indicates the percentage of radiant heat emission. The parameters above encompass a broad range of possible emission systems: from fast convectors to slow floor heating systems.

The input values for the global controller representing the μ -cogeneration devices are based on experimental data from Voorspools and D'haeseleer [Voorspools; D'haeseleer]; Peeters and D'haeseleer W. [Peeters, D'haeseleer, 2007].; and Mertens I., et al. [Mertens et al., 2005]. For both the SE and the ICE, the time "constants" for heat and electricity production, τ_p and τ_e , are actually not constant. As shown by Voorspools K. and D'haeseleer W., (2001) and Peeters and D'haeseleer (2007) they depend on the operational history of the device. The way they are implemented in the ESP-r code can be seen in Table 1, where *t* is time (s) and *fplt* is the forced part load time (s).

The ICE modeled here is a non-modulating system. The SE can modulate and is combined with an auxiliary gas burner for supplementary heat production. The ICE has an electrical output that in steady state equals 46% of the thermal capacity; for the SE this ratio is 14%.

	SE	ICE
Forced part load time $fplt$ (s)	200	-
τ_t (s)	$fplt + \left(\frac{400 \cdot t}{4 \cdot 3600}\right)$	$120 + \left(\frac{2400 \cdot t}{4 \cdot 3600}\right)$
τ_c (s)	$fplt + \left(\frac{500 \cdot t}{4 \cdot 3600}\right)$	$fplt + \left(\frac{120 \cdot t}{4 \cdot 3600}\right)$
Minimum time on (s)	240	600
Lock out time (s)	240	600

Table 1: Implemented characteristics of both SE and ICE.

RESULTS

The first aspect considered here is the influence of the limitations and characteristics of the μ -cogeneration systems ICE and SE on the optimal emitter. Figure 5 shows the net heat emission for the ICE simulations plotted against $T_{e,ref}$. This clearly shows that convective heat emitters result in a higher energy consumption compared to emitters with a higher radiant output. The upper points in this graph (greater heating requirements) represent the simulation cases with highly convective heat emitters. The explanation for this is that the sensed condition in these simulations is a mix of 50% radiant temperature and 50% air temperature. So purely convective heating emitters will need to sustain higher air temperatures and hence consume more energy than alternative mixed convective/radiant devices. An increasing time constant worsens the picture for this type of emitters, as they increase the overall average indoor temperature even further.

For a higher $T_{e,ref}$, the absolute difference between convective and radiant emitters is smaller.

The results for the SE are similar, although slightly higher energy outputs have been noticed there. The reason is the modulating regime which results in less on/off switching and consequently fewer lock out times. The longer operational times result in a higher average indoor temperature for the SE, explaining the higher net energy demand.

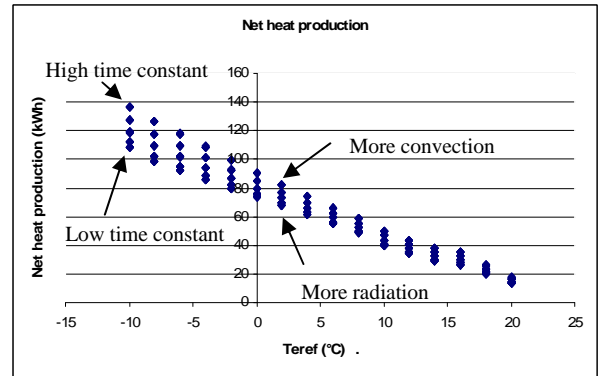


Figure 5: Net heat production as a function of the outdoor temperature for the ICE for the different heat emitters.

The next aspect considered is the influence of a given set of heat emitter characteristics on the performance of a μ -cogeneration device. The performance indicators considered here are the fuel utilisation factor⁴, the thermal performance α_{th} and the electrical performance α_{el} . The fuel utilisation factor is defined by:

$$FuelUtilisationFactor = \left(\frac{Q_{th} + Q_{el}}{PE} \right) \quad \text{Equation 2}$$

where

- Q_{th} = thermal energy produced
- Q_{el} = electrical energy produced
- PE = primary energy consumed.

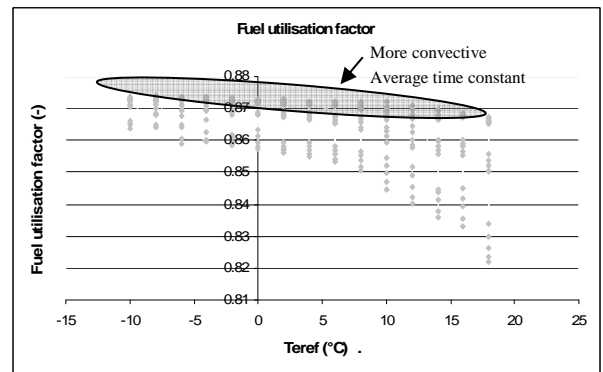


Figure 6: Fuel utilisation factor for SE as a function of $T_{e,ref}$, for the different heat emitters.

⁴ This is the sometimes referred to as “total efficiency”, referring to the first law of thermodynamics. It ignores the “quality” of the energy or “exergy”; and is to be distinguished from the exergetic efficiency, based on the second law of thermodynamics. This is the reason why we avoid the word “efficiency” here.

Figure 6 shows the fuel utilization factor as a function of $T_{e,ref}$; As would be expected, the fuel utilization factor decreases with decreasing heat demands. The reason is twofold:

- a longer time off between two operational periods has a negative influence on the time constant of the μ -cogeneration system, As can be seen in Table 1; and
- the impact of start up inefficiencies is higher in case of shorter operational periods.

In these simulations, a heat emitter with an average time constant of approximately 100 seconds seems to have the best fuel utilization ratio. Two effects can explain this:

- a higher heat emitter time constant results in higher indoor temperatures during set back; and
- a low heat emitter time constant reduces the switched-off time between two 'on'-periods, resulting in lower time constants for the μ -cogeneration system (see Table 1) .

The fuel utilization ratio for the highly convective systems equals that for the radiant systems in case of a low $T_{e,ref}$. This due to the higher heat demand for the convective systems. This higher heat demand during colder days results in a decreased cycle frequency for the μ -cogeneration device, compared to the case of average or warm outdoor conditions.

As can be seen in Figure 7, the slope of the line representing the fuel utilization factor and the one representing the thermal efficiency α_{th} , (defined according to equation 3) are very similar.

$$\alpha_{th} = \frac{Q_{th}}{PE} \quad \text{Equation 3}$$

The effects of the choice of the emitter are even more pronounced in case of an ICE, as its cycling frequency is higher due to its non-modulating thermal output. For strongly varying heat demands, higher time constant radiant emitters will result in a lower cycling frequency and better performance.

In Figure 7 the electrical efficiency α_{el} , defined according to equation 4, is shown as well.

$$\alpha_{el} = \frac{Q_{el}}{PE} \quad \text{Equation 4}$$

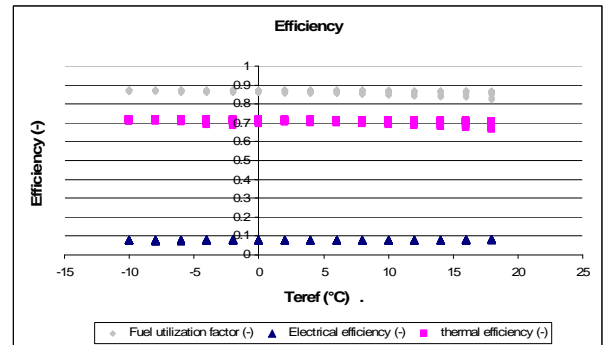


Figure 7: Efficiencies for SE as a function of $T_{e,ref}$.

The electrical efficiency slightly decreases with increasing $T_{e,ref}$. This is due to the lower load and thus shorter working hours of the μ -cogeneration system in case of warmer outdoor conditions. This results in a higher impact of the start up inefficiencies. With the time constant for electricity production being higher than the one for production of thermal energy, the weight of this start-up effect is more pronounced in the results for the electrical performance of the SE.

The decrease is also observed in the electrical performance of the ICE. But the results there have to be interpreted with care, as the effect of an increasing cycling frequency due to its fixed thermal power, might overrule any other effects. Due to the lower time constant for the electrical output, τ_{el} , compared to τ_{th} , the effects of limited switch-on periods are less pronounced in the electrical efficiency than when considering the thermal performance.

Note that the simulations performed are for constant artificial step-wise outdoor conditions. In case of fluctuating outdoor temperatures, modulating μ -cogeneration systems will outperform the non-modulating systems. The capacity of the non-modulating ICE, dimensioned for the high heat demands of cold days, is too high for a midseason day, resulting in a high cycling frequency. High thermal mass heat emitters will outperform the fast convective emitters (for both SE and ICE) because the high time constant results in a reduced cycling frequency [Peeters L. et al., 2007]. Also the installation of a storage tank can reduce the cycling frequency and thus improve the performance of the μ -cogeneration [Haeseldonckx D. et al., 2007].

CONCLUSIONS

This paper argues that thermal comfort standards developed for offices and public buildings are not satisfactory when used for residential buildings, the

reason being the widely available possibilities to adapt the thermal environment.

Based on the literature, new guidelines have been set up with an outdoor temperature dependent comfort temperature and an asymmetrically distributed 10%-PPD zone around that.

The performance of different emission systems for two types of μ CHP has been tested, using newly developed ESP-r controllers.

The simulations show that, for realising the same thermal comfort quality, convective emitters will result in higher heat demands. To limit this energy penalty, these emitters should have low time constants.

Both SE and ICE should be combined with convective heating systems with average time constant in case the variations in the heat demand are limited. For these situations the fuel utilization factor is the highest.

For varying, low heat demands, both μ CHPs benefit from high thermal mass emission systems with predominantly radiant output. This limits the impact of the start-ups inefficiencies on the overall performance. The effect is more pronounced for the ICE.

ACKNOWLEDGEMENTS

Special thanks to the ESRU community at the University of Strathclyde for giving me the opportunity to spend some valuable time in Glasgow and to the FWO for funding the stay.

REFERENCES

ANSI/ASHRAE 55-2004, Thermal Environmental Conditions for Human Occupancy, American Society of Heating, Refrigerating and Air-conditioning Engineers, Inc. Atlanta, USA

Clarke J., 2001, Energy simulation in building design, Butterworth Heinemann, ISBN 0 7506 5082 6

De Dear R., Brager G., 1997, Developing an adaptive model of thermal comfort and preference; Final report ASHRAE RP-884, Macquarie Research Ltd., Macquarie University, Sydney, Australia

ESRU, 2007, Released version 11.4, http://www.esru.strath.ac.uk/Programs/ESP-r_CodeDoc/esrures/comfort.F.html

Fanger P., 1970, Thermal comfort; analyses and applications in environmental engineering, McGraw-Hill Book Company, United States, ISBN 0-07-019915-9

Fountain M., Brager G., De Dear R., 1996, "Expectations of indoor climate control". Energy & Buildings, vol 24, pp 179-182

Haeseldonckx D, Peeters L, Helsen L, D'haeseleer W., 2007, The impact of thermal storage on the operational behaviour of residential CHP facilities and the overall CO2 emissions Renewable and Sustainable energy Reviews, vol. 11, pp 1227-1243

Hens H., 1995, Toegepaste bouwfysica en installaties in gebouwen : binnenmilieu, energie, verwarming, ventilatie, ACCO, Leuven, ISBN 978-90-334-6750-9 (In Dutch)

Humphreys M., Hancock M., 2007, "Do people like to feel 'neutral'? Exploring the variation of the desired thermal sensation on the ASHRAE scale". Energy & Buildings, vol. 39, pp 867-874

ISO 7730, 2005, Moderate thermal environments – Determination of the PMV and PPD indices and specification of the conditions for thermal comfort, International Organisation for standardization, Switzerland

Janssens A., Vandepitte A., 2006, Analysis of indoor climate measurements in recently built Belgian dwelling, IEA annex 41, report n° A41-T3-B-06-10, University of Ghent, Belgium, departments of Architecture

Jensen, S., 1993, Validation of Building Energy Simulation programs, Part 1 & 2, Research Report PASSYS Subgroup Model Validation and development, EUR 15115, TIL, CEC, Brussels

Kelly N., 1998, Towards a design environment for building-integrated energy systems: the integration of electrical power flow modelling with building simulation, PhD Thesis, University of Strathclyde, Glasgow

MacQueen John, 1997, 'The modelling and simulation of energy management control systems, PhD Thesis, University of Strathclyde, Glasgow

Mertens I., Mertens S., Peeters, L., D'haeseleer W.,
'Integratie van Stirlingmotor in WKK-installaties en
elektriciteitscentrales', TME/2004-2005/EE-01, 2005
(In Dutch)

Oseland N., 1994, A comparison of the predicted and
reported thermal sensation vote in homes during winter
and summer, Energy and Buildings, vol.21, pp 45-54

Oseland N., 1995, Predicted and reported thermal
sensation in climate chambers, offices and homes,
Energy and Buildings, vol 23, pp 105-115

Peeters L., D'haeseleer W., 2007, Meetcampagne
WhisrepGEN (In Dutch), IWT GBOU 020212, Applied
Mechanics and Energy Conversion, KULeuven

Peeters L., Van der Veken J., Helsen L., Hens H.,
D'haeseleer W., Sizing of boilers for residential
buildings, electronic proceedings, Clima 2007 (9th
REHVA Clima WellBeing Indoors Conference),
Helsinki, 10-14 June 2007

Peeters L., Van der Veken J., Hens H., Helsen L.,
D'haeseleer W., 2008, Control of heating systems in
residential buildings: current practice, Energy and
Buildings, accepted for publication

Van der Linden A., Boerstra A., Raue A., Kurvers S.,
De Dear R., 2006, Adaptiv etemperature limits: A new
guideline in the netherlands. A new approach for the
assesment of building performance with respect to
thermal indoor climate, Energy and Buildings, vol 38,
pp 8-17

Voorspools K., D'haeseleer W., 2001, Mini- en Micro-
WKK, Co2-project Fase 3 (In Dutch), TME/WDH/01-
01.2/FIN, Applied Mechanics and Energy Conversion,
KULeuven